

## CHAPTER II

### LITERATURE REVIEW

#### 2.1 Clay Minerals

Clay minerals are a part of a general but important group within the phyllosilicates that consist of sheets of silica tetrahedral and alumina octahedral which are held together by only weak interatomic forces between the layers. Owing to their chemical composition and crystal structure, they are divided into four main groups which are illite, smectite, vermiculite and kaolite. Among these, the one that is found to be useful in the field of polymer composites is a group of expandable clay known as smectite clay.

Smectite clay is phyllosilicates or layer silicates having a layer lattice structure in which two-dimensional oxoanions are separated by hydrated cations (Kloprogge *et al.*, 1998). Montmorillonite, which is the main constituent of bentonites, is a mainly species of smectite clay. The structure of MMT is made of several stacked layers, with a layer thickness around 0.96 nm and a lateral dimension of 100-200 nm (Lertwimolnum and Vergnes, 2005). Its crystal lattice consists of a central octahedral sheet of alumina fused between two external silica tetrahedral sheets (in such a way that the oxygens from the octahedral sheet also belong to the silica tetrahedral), as shown in Figure. 2.1 These layers organize themselves in a parallel fashion to form stacks with a regular van der Waals gap between them, called interlayer or gallery (Manias *et al.*, 2001).

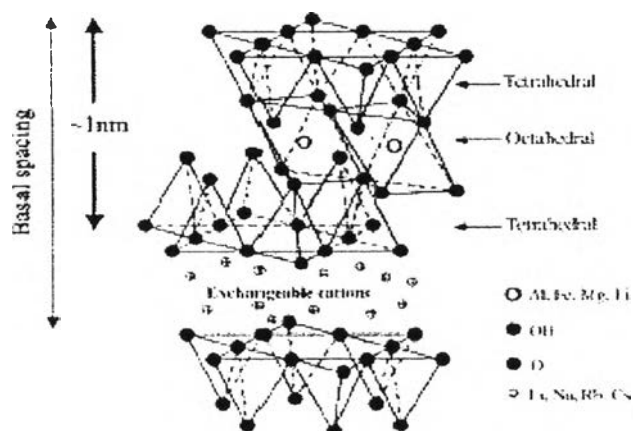


**Figure 2.1** Structure of montmorillonite.

Isomorphic substitution within the layers (for example,  $\text{Al}^{3+}$  replaced by  $\text{Mg}^{2+}$  or  $\text{Fe}^{2+}$ , or  $\text{Mg}^{2+}$  replaced by  $\text{Li}^{1+}$ ) generates negative charges that are counterbalanced by alkali and alkaline earth cations situated inside the galleries. This type of layered silicate is characterized by a moderate surface charge known as the cation exchange capacity (CEC), and generally expressed as mequiv/100 gm. This charge is not locally constant, but varies from layer to layer, and must be considered as an average value over the whole crystal (Manias *et al.*, 2001; Sinha Ray Okamoto, 2003). Thus, in order to have a successful development of clay-based nanocomposites, it is necessary to chemically modify a naturally hydrophilic silicate surface to an organophilic one so that it can be compatible with a chosen polymer matrix. Generally, this can be done through ion-exchange reactions by replacing interlayer cations with quaternary alkyl ammonium or alkylphospho-ion-exchange reactions cations with cationic surfactants such as those mentioned above render the normally hydrophilic silicate surface organophilic, thus making it more compatible with non polar polymers. These cationic surfactants modify interlayer interactions by lowering the surface energy of the inorganic component and improve the wetting characteristics with the polymer. Furthermore, they can provide functional groups .That can react with the polymer or initiate polymerization of monomers and there by improve the strength of the interface between the polymer and inorganic component (Quang and Donald, 2006).

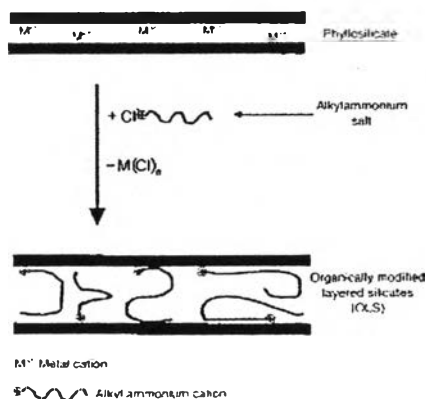


**Figure 2.2** Schematic representation of a cation-exchange reaction between the silicate and an alkylammonium salt (Quang and Donald, 2006).

In the present work, montmorillonite is a clay mineral used for the preparation of polymer-clay nanocomposites. Montmorillonite is a very soft phyllosilicate mineral that typically forms in microscopic crystals, forming clay. It is the main constituent of the volcanic ash weathering product, bentonite. The presence of these compounds can impact the industrial value of bentonite. Bentonite has unique water absorbing and swelling characteristics. These characteristics make bentonite a very desirable industrial mineral. The adsorption and ion exchange properties of clay minerals on many parameters. In addition to electrolyte concentration, pH of solution ( $H^+$  ion) controls the swelling behavior of expandable clay minerals.

In 1999, Altin *et al.* determined surface area, pore volume distribution, and porosity of montmorillonite after being exposed to aqueous solutions with various pH values. For the pH-adjusted montmorillonite, the results demonstrated that the micropore and mesopore surface areas were greatly increased by increasing pH due to increasing pH creates a more porous structure, since the interlayer repulsive force becomes dominant. Then pore volume distributions showed that lowering pH of montmorillonite reduced the mesoporous and microporous.

Thajaroen W. (2000), found in case of primary-alkylamine modified montmorillonites (MMTs), the degree of basal spacing expansion was increased with the length of hydrocarbon part in the structure of modifying agents. For quaternary-

ammonium salt modified MMTs, the same trend was obtained but the degree of interlayer expansion was lower than that of primary-alkylamine modified counterparts.

## 2.2 Porous Clay Heterostructure (PCH)

A variety of ordered mesoporous materials have been synthesized by surfactant-templated methods. Porous clay heterostructure (PCH) is a recent class of solid porous materials formed by the intercalation of surfactant within the intragalleries of clays. Various types of expandable clay could be employed such as hectorite, vermiculite, synthetic saponite and montmorillonite for the synthesized of these highly porous clays.

Pichowicz and Mokaya, 2001 prepared Porous clay heterostructures (PCHs) from suitably acid-activated montmorillonite clays; the higher acidity arises from Bronsted acid sites generated by acid treatment of the clay prior to its use as a host for PCH formation. The results of PCHs and PAACHs (porous acid activated clay heterostructures) are the PCH samples have surface area of 800 m<sup>2</sup>/g while the acid-activated clay derived samples have higher surface area of 915 m<sup>2</sup>/g for PAACH which is derived from acid activated clay using octylamine and 951 m<sup>2</sup>/g for PAACH which is derived from acid activated clay using decylamine. The surface areas of the present materials are generally higher than that of fluorohectorite-PCH but comparable to those of saponite and montmorillonite derived PCHs.

Polverejan *et al.*, (2002) prepared by the post synthesis grafting of aluminum into the meso structured intra gallery silica framework of a PCH precursor derived adsorption, from a synthetic saponite clay. Elemental analyses, powder X-ray diffraction,

N<sub>2</sub> adsorption and <sup>27</sup>Al MAS NMR spectroscopy were used to characterize the reaction products, which designated Al-SAP/PCH. Depending on the choice of aluminum reagent (AlCl<sub>3</sub> or NaAlO<sub>2</sub>), the Al-SAP/PCH derivatives exhibited basal spacings of 32-34.8 Å, BET surface areas of 623-906 m<sup>2</sup>/g, pore volumes of 0.32-0.45 cm<sup>3</sup>/g, and pore sizes in the large micropore to small mesopore range (14-25 Å).

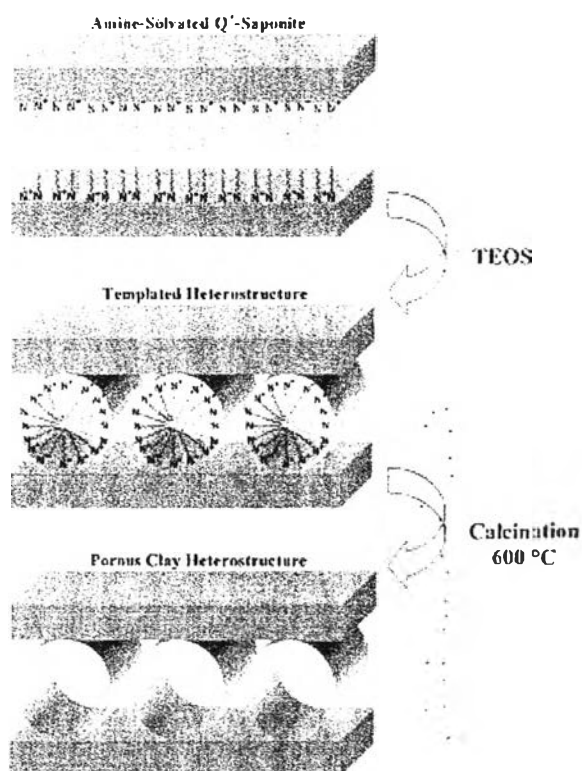


**Figure 2.3** Schematic representation of porous clay hetero structure (PCH) formation through surfactant-directed assembly of mesostructured silica in the galleries of a quaternary ammoniumion-exchanged layered silicate co-intercalated by an electrically neutral amine cosurfactant. (Polverejan *et al.*, 2002).

Polverejan *et al.* (2000) prepared porous clay heterostructures within the galleries of synthetic saponite clays with targeted layer charge densities in the range  $x = 1.2-1.7$   $e^-$  units per  $Q^+ [Mg_6](Si_{8-x}Al_x)O_{20}(OH)_4$  unit cell. The CEC value increase in proportional to the aluminum content of the clays. All three saponites were used to assemble porous clay heterostructures that were denoted SAP1.2-, SAP1.5-, and SAP1.7-PCH, respectively. The removal of the intragallery mixture of neutral alkylamine and quaternary ammonium ion surfactant (Q+) by calcination afforded PCH intercalates with basal spacings of 33-35 Å. The BET specific surface areas progressively decreased with increasing aluminum loading from 921 to 797  $m^2 g^{-1}$  and the framework pore volumes decreased from 0.44 to 0.37  $cm^3 g^{-1}$ . Moreover, these materials exhibited the framework pore sizes were in the supermicropore to

small mesopore region 15-23 Å as can be seen in TEM image (Figure 2.4). In 2000, they synthesized acid-functionalized porous clay heterostructure from synthetic saponite through postsynthesis grafting reactions using  $\text{AlCl}_3$  and  $\text{NaAlO}_2$  as alumination agents under acid and basic condition, respectively. The amount of tetrahedral aluminum incorporated into the saponite gallery structure is correlated with the concentration of aluminum in the grafting solution. However, some loss of gallery mesostructure occurred at higher aluminum loadings (e.g.,  $\text{Si}/\text{Al} = 5$ ) with sodium aluminate. Depending on the choice of aluminum reagent ( $\text{AlCl}_3$  or  $\text{NaAlO}_2$ ), the Al-SAP/PCH derivatives exhibited basal spacings of 32-34.8 Å, BET surface areas of 623-906  $\text{m}^2/\text{g}$ , pore volumes of 0.32-0.45  $\text{cm}^3/\text{g}$ , and pore sizes in the large micropore to small mesopore range (14-25 Å).

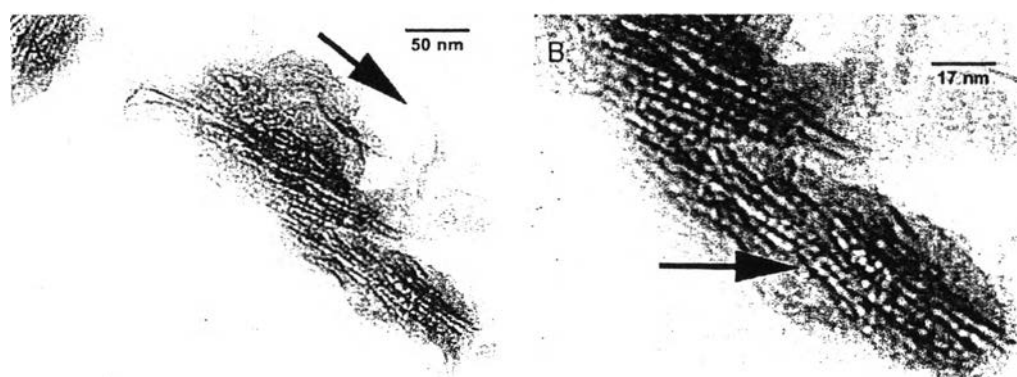


**Figure 2.4** TEM image saponite heterostructure (Polverejan *et al.*, 2000).

Benjelloun *et al.* (2001) studied the cationic exchange capacities (CECs) of two porous clay heterostructures (PCHs), derived from natural montmorillonite (PMH) and synthetic saponite (PSH). Three methods for the formation of  $\text{NH}_4^+$ -exchanged PCH forms are describe and evaluated: (1) adsorption of ammonia under a gas flow on calcined and extracted PCHs in acidified methanol; (2) direct exchange in  $\text{NH}_4\text{Cl}$  solutions; (3) solvent extraction with  $\text{NH}_4\text{Ac}/\text{EtOH}/\text{H}_2\text{O}$ . The obtained ammonium containing materials are subsequently exchanged for  $\text{K}^+$  cations in aqueous solution in order to determine the CEC of the PCH solids. Several extraction media were tested for their efficiency in extracting the hexadecyltrimethylammonium surfactant from the PCH precursor. The best results were obtained with

methanol:water mixture with 9:1 vol%. The resulting extracted materials had a higher specific surface area and porosity and even a slightly narrower pore size distribution than the calcined ones with maxima of 997 m<sup>2</sup>/g. and 0.76 cm<sup>3</sup>/g for montmorillonite PCH (PMH) and 1118 m<sup>2</sup>/g and 0.97 cm<sup>3</sup>/g for saponite PCH (PSH).

### 2.3 Polylactide or Polylactic acid (PLA)

Polylactides or poly (lactic acid) (PLA) is a linear aliphatic thermoplastic which can either be synthesized by condensation of lactic acid or ring opening polymerization of lactide which is the diester of lactic acid. Lactic acid is a chiral organic acid which mainly occurs in the L-form. It is produced by fermentation of dextrose which itself is gained from annually renewable resources like corn (Bax and Mussig, 2008). Among the renewable source-based biodegradable plastics, PLA is one of the most promising materials since it is thermoplastic, biodegradable, biocompatible and has high-strength, high-modulus and good processability (Drumright *et al.*, 2000; Garlotta, 2001).

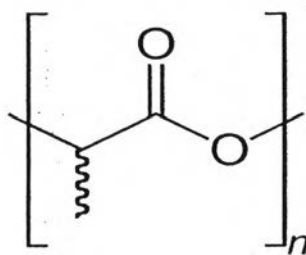


**Figure 2.5** The skeletal formula of polylactic acid ([www.wikipedia.com](http://www.wikipedia.com)).

Kikkawa *et al.* (2004) studied effect of water on the surface molecular mobility of Poly ( lactide ) thin films with 300 nm thickness by an atomic force microscopy. Two types of PLAs were applied for the experimental samples as uncrystallizable PLA (uc-PLA) and crystallizable PLA (c-PLA). The amorphous region around the hexagonal crystal in a partially crystallized c-PLA thin film was

completely degraded at 20°C within 15 min, whereas the crystalline region remained unchanged in the presence of proteinase K. Thus, the amorphous region around the crystal was preferentially degraded by the enzyme at a fast rate. The surface glass-transition temperature of the amorphous uc-PLA (PLDLA) thin film was determined from the friction and temperature curves. The glass-transition temperature (58°C) for uc-PLA in water was lower than that (70°C) in vacuum conditions, suggesting that water molecules function as a plasticizer and enhance the molecular mobility of PLA molecules on the surface of PLAs. Friction force measurement was also performed on the surface of the amorphous c-PLA (PLLA) thin film as a function of temperature. In addition, the morphological change of c-PLA during heating process was observed by AFM. A cold crystallization temperature for c-PLA was decreased in the presence of water compared with that under vacuum conditions.

Due to high production costs, in the early stages of its development PLA was used in limited areas, such as preparation of medical devices (bone surgery, suture, and chemotherapy, etc.). Since production cost has been lowered by new technologies and large-scale production, the application of PLA has been extended to other commodity areas such as packaging, textiles and composite materials (Drumright, Gruber and Henton, 2000; Garlotta, 2001).

#### **2.4 Polymer-Clay Nanocomposites**

Polymer-clay nanocomposites exhibit outstanding properties that are synergistically derived from the organic and inorganic components. They exhibit superior mechanical properties, reduced gas permeability, improved solvent resistance and enhance ionic conductivity (Galgali *et al.*, 2001). Several methods have been considered to prepare polymer-clay nanocomposites. They include four main processes [Oriakhi, 1998.]:

1. Exfoliation-adsorption: the clay is exfoliated into single layers using a solvent in which the polymer (or a prepolymer in case of insoluble polymers such as polyimide) is soluble. The polymer then adsorbs onto the delaminated sheets and when the solvent is evaporated (or the precipitation of mixture), the sheets reassemble, sandwiching the polymer to form, in the best case, an ordered multilayer



structure. Under this process are also gathered the nanocomposites obtained through emulsion polymerization where the silicate clay is dispersed in the aqueous phase.

2. In situ intercalative polymerization: the silicate clay is swollen within the liquid monomer (or a monomer solution) so the polymer formation can occur in between the intercalated sheets. Polymerization can be initiated either by heat or radiation, by the diffusion of a suitable initiator or by an organic initiator or catalyst fixed through cationic exchange inside the interlayer before the swelling step by the monomer.

3. Melt intercalation: the silicate clay is mixed with the polymer matrix in the molten state. Under these conditions and if the layer surfaces are sufficiently compatible with the chosen polymer, the polymer can crawl into the interlayer space and form either an intercalated or an exfoliated nanocomposite. This method has great advantages: first, this method is environmentally benign due to the absence of organic solvents. Second, it is compatible with industrial process, such as extrusion and injection molding. The melt intercalation method allows the use of polymers which were previously not suitable.

4. Template synthesis: where the silicates are formed in situ in an aqueous solution containing the polymer and the silicate building blocks has been widely used for the synthesis of double-layer hydroxide-based nanocomposites but is far less developed for layered silicates. In this technique, based on self-assembly forces, the polymer aids the nucleation and growth of the inorganic host crystals and gets trapped within the layers as they grow.

Nanocomposite structures depending on the nature of the components used (layered silicate, organic cation and polymer matrix) and the method of preparation, three main types of composites may be obtained when layered clay is associated with a polymer (Figure 2.6). When the polymer is unable to intercalate between the silicate sheets, a phase separated composite (Figure 2.6a) is obtained, whose properties stay in the same range as traditional microcomposites. Beyond this classical family of composites, two types of nanocomposites can be recovered. Intercalated structure (Figure 2.6b) in which a single (and sometimes more than one) extended polymer chain is intercalated between the silicate layers resulting in a well ordered multilayer morphology built up with alternating polymeric and inorganic

layers. When the silicate layers are completely and uniformly dispersed in a continuous polymer matrix, an exfoliated or delaminated structure is obtained (Figure 2.6c) (Alexandre and Dubois., 2000).

Depending on the strength of interfacial interactions between the polymer matrix and layered silicate (modified or not), three different types of PLS nanocomposites are thermodynamically achievable, as shown in Figure. 2.7 (Sinha and Okamoto, 2003).

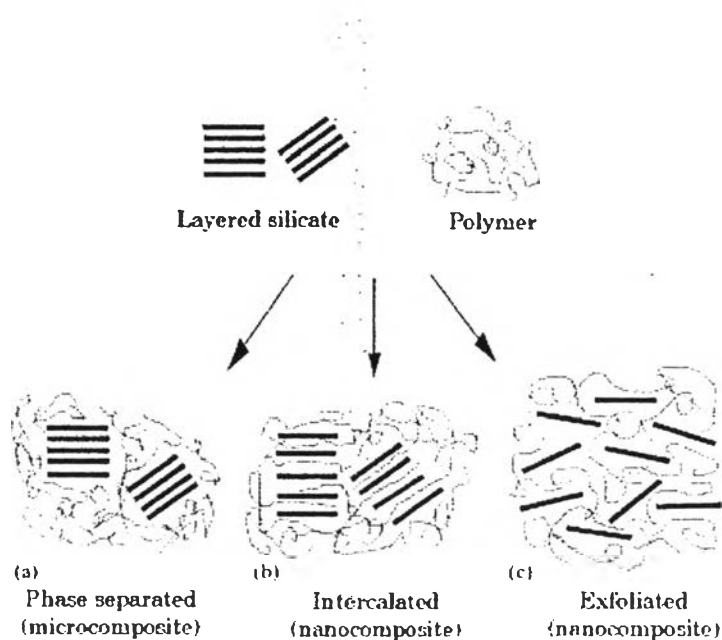


**Figure 2.6** The schematic of different types of composite arising from the interaction of layered silicates and polymers: (a) phase-separated microcomposite; (b) intercalated nanocomposite and (c) exfoliated nanocomposite (Alexandre and Dubois., 2000).

- *Intercalated nanocomposites*: in intercalated nanocomposites, the insertion of a polymer matrix into the layered silicate structure occurs in a crystallographically regular fashion, regardless of the clay to polymer ratio. Intercalated nanocomposites are normally interlayer by a few molecular layers of polymer.

- *Flocculated nanocomposites*: conceptually this is same as intercalated nanocomposites. However, silicate layers are some times flocculated due to hydroxylated edge–edge interaction of the silicate layers.

- *Exfoliated nanocomposites*: in an exfoliated nanocomposite, the individual clay layers are separated in a continuous polymer matrix by an average distances that depends on clay loading. Usually, the clay content of an exfoliated nanocomposite is much lower than that of an intercalated nanocomposite.

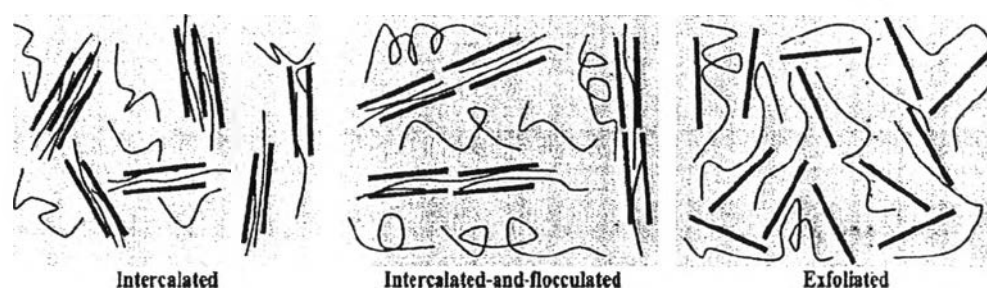


**Figure 2.7** Schematically illustration of three different types of thermodynamically achievable polymer/layered silicate nanocomposites (Sinha and Okamoto, 2003).

Many researches efforts focus on the preparation of polypropylene-clay nanocomposites. But PP does not include polar groups in its backbone; it was thought that the homogeneous dispersion of the silicate layers in PP would not be realized. Hence, it is frequently necessary to use a compatibilizer such as maleic anhydride modified polypropylene (PP-g-MA). There are two important factors to achieve the exfoliation of the clay layer silicates: (1) the compatibilizer should be miscible with the polypropylene matrix, and (2) it should include a certain amount of polar functional groups in a molecule. Generally, the polypropylenes modified with maleic anhydride (MA) fulfill the two requirements and are frequently used as compatibilizer for polypropylene nanocomposites. However, they have mechanical properties lower than the native polypropylene, due to chain scission during grafting (Lertwimolnum and Vergnes., 2005).

Sinha Ray *et al.* (2002) described the preparation, characterization, material properties, and biodegradability of polylactide (PLA)-layered silicate nanocomposite.

Montmorillonite modified with trimethyl octadecylammonium cation was used as an organically modified layered silicate (OMLS) for the nanocomposite preparation. WAXD and TEM analyses respectively confirmed that silicate layers of the montmorillonite were intercalated and nicely distributed in the PLA-matrix. The material properties of neat PLA improved remarkably after nanocomposite preparation. The biodegradability of the neat PLA and corresponding nanocomposite was studied under compost, and the rate of biodegradation of neat PLA increased significantly after nanocomposite preparation. And this research described polylactide (PLA)-clay nanocomposites loaded with 3 wt% organomodified montmorillonite and PLA-clay microcomposites containing 3 wt % sodium montmorillonite were prepared by melt blending and investigated the morphology and thermal properties of the nanocomposites and microcomposites and compared them with unfilled PLA, keeping the same thermomechanical history. The influence of the processing temperature on the structural characteristics of the investigated systems was determined. The investigations were performed with differential scanning calorimetry (DSC), thermogravimetric analysis (TGA), X-ray diffraction (XRD), size exclusion chromatography (SEC), and polarized light microscopy (LM). XRD showed that the good affinity between the organomodified clay and the PLA was sufficient to form intercalated structure in the nanocomposite. The microcomposite featured a phase-separated constitution. DSC and LM studies showed that the nature of the filler affected the ordering of the PLA matrix at the molecular and supermolecular levels. According to TGA, the PLA-based nanocomposites exhibited improvement in their thermal stability in air. Reduced flammability, together with char formation, was also observed for nanocomposites, compared to the microcomposites and pure PLA (M. Pluta *et al.*, 2002).

Maiti *et al.*, (2002) The nanocomposites is polylactide-clay nanocomposites which mixed by twin screw extruder. In the preparation of polymer/clay nanocomposites, organoclay plays an important role in lipophilizing and dispersing the clay into less polar polymer matrixes. Organic modifiers of various chain lengths were examined in different types of clays, smectite, montmorillonite (MMT), and mica, to prepare their corresponding organoclays. The layered structure and gallery spacing of organoclays and polylactide (PLA) nanocomposites shows that, with a

modifier of the same chain length, the gallery spacing of the organoclay was largest for mica and smallest for smectite because of the higher ion-exchange capacity of mica and physical jamming of the modifier due to a restricted conformation at the core part of the clay of larger size. The increment of the modulus in a smectite nanocomposite, compared to that of PLA, is higher than MMT or mica nanocomposite due to better dispersion in a smectite system for the same clay loading. Being a well-dispersed system, smectite nanocomposites have better gas barrier properties than the MMT or mica systems, which are larger in size but stacked in nature in their nanocomposites. A new idea for obtaining porous ceramic material from layered silicate/polymer nanocomposites by burning is unveiled using various clays and the mechanism of their formation is elucidated

Solarski *et al.*(2007) studied thermal, mechanical, shrinkage and fire properties of (Plasticized) polylactide-clay nanocomposite textile. This experiment has various quantities of Cloisite<sup>®</sup> 30B (from 1% to 4% in weight) which is the additive used for the preparation of the PLA nanocomposites. The surfactant of the C30B is a methyl tallow alkyl bis-2-hydroxyethyl quaternary ammonium cation. C30B is delivered in the shape of a fine powder have been added to a polylactide matrix by melt blending to produce polylactide-based nanocomposites. The interactions between the carbonyl functions of PLA chains and hydroxyl functions of the alkyl ammonium surfactants surface-covering MMT nanoplatelets seem to improve the dispersion of this organo-clay in a PLA matrix, contrary to other kinds of MMT without hydroxyl functions on the surfactant then; these blends have been melt-spun to produce multifilaments yarns. It is demonstrated that it is necessary to use a plasticizer to spin a blend with 4% in weight of Cloisite<sup>®</sup> 30B. The properties of these yarns have been studied (dispersion of the clay, thermal, mechanical and shrinkage properties). A decrease of the tensile properties is observed when the quantity of Cloisite<sup>®</sup> 30B increases, but an improvement of the thermal and shrinkage properties is highlighted. These multifilaments have been knitted and the flammability studied using cone calorimeter at 35 kW/m<sup>2</sup>. A strong decrease, up to 38%, of the heat release rate has been measured.

Gu *et al.* (2007) studied about the linear and nonlinear shear rheological behaviors of polylactide (PLA)-clay (organophilic-montmorillonite) nanocomposites

ต้นฉบับ หน้าขาดหาย

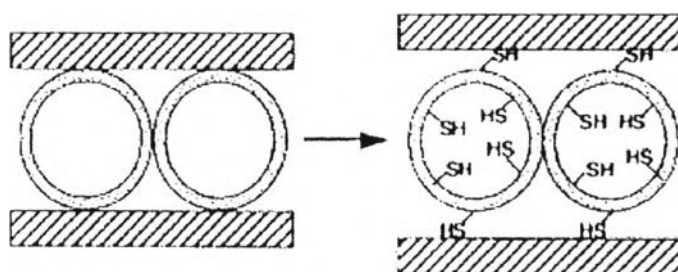


**Figure 2.8** Grafting of mercaptopropylsilane groups to the inner and outer walls of mesostructural silica intercalated in smectite clay (Mercier and Pinnavaia, 1998).

The adsorption properties of PCH have been considered in a number of studies, particularly when considering adsorption process as the recovery of volatile organic compounds or the enrichment of the more valuable fractions of natural or land fill gas. In 2004, Pires *et al.* prepared porous materials from a natural smectite by the gallery templated approach, using a quaternary ammonium cation (CTAB) and neutral amines with different chain length (octylamine and decylamine). The materials prepared in this work, after calcination at  $650^{\circ}\text{C}$ , had  $A_{\text{BET}}$  values in the range of  $600\text{--}700\text{ m}^2\text{g}^{-1}$  and micropore volumes near  $0.3\text{ cm}^3\text{g}^{-1}$ . Furthermore, the samples presented pores with widths in the transition between micro to mesopores. The possibility of using such materials as adsorbents of volatile organic compounds, due to their textural and hydrophobic characteristics, was studied by the adsorption of ethanol and methyl ethyl ketone and water for comparison. The data from the adsorption showed that particularly one sample where decylamine was used in the synthesis, has interesting properties regarding the adsorption of VOCs.

Pinto *et al.* (2005) prepared composite adsorbent material supporting pillared clay in polyurethane foam for application in air filtering systems combining the ability of retaining noxious volatile organic compounds (VOC). The pillared clay was obtained from a natural montmorillonite by pillaring with aluminium oxide pillars. Adsorption isotherms of nitrogen and toluene were determined to evaluate the adsorption capacity of the adsorbent material before and after being support in the polyurethane. The result indicated that the pillared clay presented a decrease of about

97% in nitrogen adsorption capacity and also pronounced decrease in the toluene adsorption capacity. In 2006, they also studied the thermal regeneration of the composite material and the recycling of the adsorbents. The results showed a decrease in the adsorption capacity about 60% after regeneration process. However, the recycling of the adsorbent materials was possible since the adsorption capacity of the recycled material was in fact similar to the initial material before being support in the polyurethane.

## 2.6 Magnetic Properties

Magnetic materials are one of the most prominent classes of functional materials. They are mostly inorganic, metallic or ceramic in nature and typically multi component when used in applications such as alloys or intermetallic phases. Their structure can be amorphous or crystalline with grain sizes ranging from a few nanometers (as in high-end nanocrystalline soft magnetic materials) to centimeters (as in grain-oriented transformer steels). They are available as powders, cast, sintered or composite materials, ribbons or even thin films and find a huge variety of applications in transformers, motors, generators, medical system sensors, and microelectronic devices. Empirically, materials are classified according to their response to an applied magnetic field, i.e. the magnetization induced by the external field. More fundamental understanding results from considering the microscopic mechanisms that determine the behavior of materials in the magnetic field. The types of magnetic are diamagnetism, paramagnetism and ferromagnetism.

1. Diamagnetism is a property of all materials. It results from an additional orbital angular momentum of electrons induced in a magnetic field. In analogy to the induction of eddy currents in a conductor it manifests itself as a magnetization oriented in the opposite direction to the external field.

2. Paramagnetism means a positive magnetic susceptibility, i.e. the induced magnetization is along the direction of the external magnetic field. It is observed in materials which contain atoms with nonzero angular momentum, e.g. transition metals. The susceptibility scales with  $1/T$  (Curie is law). Paramagnetism is also found in certain metals as a consequence of the spin of conduction electrons. The



related susceptibility is essentially independent of temperature. The paramagnetic susceptibility is generally several orders of magnitude larger than the diamagnetic component; therefore, diamagnetism is not observable in the presence of paramagnetism.

3. Ferromagnetism describes the fact that certain solid materials exhibit a spontaneous magnetization,  $M_S$ , even in the absence of an external magnetic field. It is a collective phenomenon resulting from the spontaneous ordering of the atomic magnetic moments due to the exchange interaction among the electron spins. It is observed in a few transition metals where itinerant electrons play the essential role for the exchange coupling mechanism, but also in their oxides, halides etc., where the exchange interaction is mediated by localized electrons of oxygen, sulfur etc. atoms located between neighboring metal atoms (indirect exchange, superexchange). Many ferromagnetic objects do not show a net magnetization without an external magnetic field. This is a consequence of magnetic domains, which are formed to reduce the energy connected with the dipolar fields. When an external magnetic field is applied domains gradually vanish due to the motion of domain walls and rotation of the magnetization inside the domains. These processes are partly reversible and irreversible. In sufficiently high fields technical saturation is achieved. The corresponding saturation magnetization, however, must not be mistaken for the spontaneous magnetization. The reason is that, at any temperature  $T > 0$ , an external field will increase the magnetization above the spontaneous value inside the domains by suppression of spin waves (the para-process). Hence, the experimental determination of the spontaneous magnetization in general requires a specific extrapolation of high field data to zero fields (Harada *et al.*)

Ferroelectricity is the electric analogue to ferromagnetism. Ferroelectric materials, such as barium titanate, exhibit spontaneous polarization without the presence of an external electric field. Ferroelectrics can be utilized for memory devices in computers, etc. The area within a hysteresis loop is proportional to the energy per unit volume that is dissipated once a full field cycle has been completed (Hummel *et al.*, 2004).

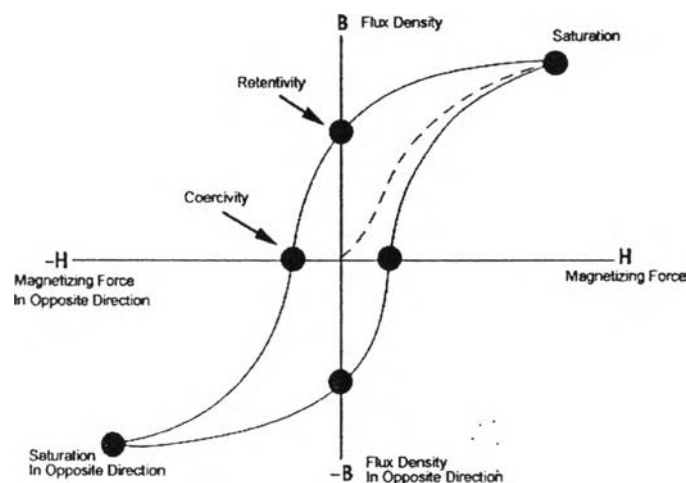


**Figure 2.9** The schematic representation of a hysteresis loop for a ferroelectric material in an electric field (Hummel *et al.*,2004).

Many researches efforts focus on the preparation of the magnetite particles. The preparation of copolymer-stabilized aqueous-based magnetite nanoparticles in research of water dispersible magnetite nanoparticles stabilized with poly (ethylene glycol) methyl ether-b-poly ( $\epsilon$ -caprolactone) copolymers and its drug-released behavior which used  $\text{FeCl}_3$  (1.66 g) in deionized water (20 ml) and  $\text{FeCl}_2 \cdot 4\text{H}_2\text{O}$  (1.00 g) in deionized water (20 ml) were mixed with stirring. Black precipitant was observed once 25%  $\text{NH}_4\text{OH}$  (20 ml) was added into the solution, indicating the formation of magnetite nanoparticles. The dispersion was continuously stirred for another 30 min to complete the reaction. The dispersion was centrifuged at 3000 rpm for 20 min and the aqueous supernatant was discarded. Oleic acid solution in hexane (2.0 ml in 20 ml hexane) was then introduced into the magnetite dispersion with stirring. The dispersion was concentrated by evaporating hexane to obtain a black thick liquid of concentrated magnetite in hexane. Precise concentration of magnetite in the dispersion was determined by atomic absorption spectroscopy technique (AAS). To prepare the copolymer-stabilized nanoparticles, 20 ml of the dispersion was introduced into various concentrations of copolymer solutions (5%, 1%, 0.5%, 0.1%, 0.01% and 0.001% w/v of the copolymer solutions) in deionized water (20 ml). The aqueous-layer dispersions were then sonicated for 4 h, followed by

centrifugation at 3000 rpm for 20 min to remove feasible agglomeration ( Meerod *et al.* ).

Next, Ferric chloride hexahydrate ( $\text{FeCl}_3 \cdot 6\text{H}_2\text{O}$  > 99%) and ferrous chloride tetrahydrate ( $\text{FeCl}_2 \cdot 4\text{H}_2\text{O}$  >99%) are used as iron sources, and aqueous ammonia is used as the precipitator. Distilled water is used as the solvent. The solution of  $\text{FeCl}_3$  and  $\text{FeCl}_2$  was mixed with certain molar ratio. The corresponding phase  $\text{NH}_4\text{OH}$  was slowly injected into the mixture of  $\text{FeCl}_3$  and  $\text{FeCl}_2$  under vigorous stirring. After precipitation, the  $\text{Fe}_3\text{O}_4$  particles were repeatedly washed and filtered before drying at room temperature in air atmosphere to form powders. Before the reaction,  $\text{N}_2$  gas was flown through the reaction medium to prevent possible oxidation. The reaction was operated in a closed system to provide a nonoxidation environment. Otherwise,  $\text{Fe}_3\text{O}_4$  might also be oxidized which means the suspension will turn from black to yellow and will affect the purity of the final production. The  $\text{Fe}_3\text{O}_4$  nanoparticles prepared by co-precipitation were dried at room temperature in air atmosphere to form a powder, which they called the powder sample.  $\text{Fe}_3\text{O}_4$  powder, 0.0122g, was put into 6 ml distilled water to form the aqueous solution and then HCl added to the aqueous solution to a pH of 2. After ultrasonic shocking of the aqueous solution, the  $\text{Fe}_3\text{O}_4$  nanoparticles were well dispersed in the distilled water and then the solution formed, which they called the dispersed suspension sample. The structural properties of  $\text{Fe}_3\text{O}_4$  nanoparticle powders were analyzed by X-ray diffraction , the mean size and morphologies of  $\text{Fe}_3\text{O}_4$  particles were observed by transmission electron microscopy and a vibrating sample magnetization) was used to evaluate the magnetic parameters (Liu *et al.*, 2002).

Synthesis of magnetic nanoparticles's graft polymerization synthesis and application of magnetic  $\text{Fe}_3\text{O}_4$  /polyacrylic acid composite nanoparticles synthesized  $\text{Fe}_3\text{O}_4$  nanoparticles, the mixture of  $\text{FeCl}_3$  (0.5M,70mL),  $\text{FeSO}_4$  (0.5M,40mL),and parafn liquid (5mL) was prepared under Ar protection. The molar ratio of  $\text{FeCl}_3$  to  $\text{FeSO}_4$  was 1.75 to 1.10 mL of ammonia aqueous solution was then quickly charged into the solution with vigorously stirring, followed by more ammonia aqueous solution being dropped into the mixture slowly with stirring until the pH value of the solution reached 9. Thereafter, the solution was kept stirring for additional 30 min under Ar protection. The resulted black mixture was aged for one night. Finally, the

precipitate was collected by filtration and washed three times with distilled water and ethanol alcohol, respectively (Hong *et.al*, 2007).

Preparation of magnetite ( $\text{Fe}_3\text{O}_4$ ) nanoparticles in research of synthesis and properties of magnetite/poly (aniline-co-8-amino-2-naphthalene sulfonic acid) nanocomposites used  $\text{FeCl}_2 \cdot 4\text{H}_2\text{O}$  (0.158 g) and  $\text{FeCl}_3 \cdot 6\text{H}_2\text{O}$  (0.268 g) were dissolved in 45 ml of deionized water. Aqueous ammonia (1.2 ml, 28 wt%) was added into the solution of mixed iron salts and the solution was purged with nitrogen gas. The reaction was allowed to proceed for 1.5 hr. with stirring. A black precipitate was obtained. The precipitate was removed by centrifugation at 4000 rpm for 30 min and washed repeatedly under vacuum with distilled water. The magnetite particles thus obtained were dried at  $60^\circ\text{C}$  under vacuum for 6 hrs. (Raghava Reddy *et al.*, 2007).

P. Saravanan *et.al*, (2002) studied effect of substitution of Mn ion on magnetic properties of  $\text{Fe}_3\text{O}_4$  nanocrystallites.  $\text{Fe}_3\text{O}_4$  magnetic colloids were produced by the chemical co-precipitation method, i.e., mixing an acidic solution of  $\text{FeCl}_2 \cdot 4\text{H}_2\text{O}$ ,  $\text{FeCl}_3 \cdot 6\text{H}_2\text{O}$  and  $\text{MnCl}_2 \cdot 4\text{H}_2\text{O}$  with a concentrated alkali solution of pH around 12 at  $\sim 90^\circ\text{C}$ . Reactions were carried out using Mn ion concentration of 0 wt%, 6 wt%, 12 wt% and 18 wt% and with a molar ratio of  $\text{Fe(II)/Fe(III)} = 0.5$ . The precipitates liquid was removed from the precipitate by decantation. The cationic colloidal nanoparticles were obtained by neutralizing the anionic charges on the colloidal nanoparticles by adding dilute hydrochloric acid. The black Mn substituted  $\text{Fe}_3\text{O}_4$  precipitates obtained were strongly attracted to a magnet. The results show that the particles of  $\text{Fe}_3\text{O}_4$  colloids have an average diameter about 8 nm and the particle sizes however increased slightly upon Mn doping. And the  $M_s$  value of  $\text{Fe}_3\text{O}_4$  nanocrystals increases with the small Mn doping and tends to decrease with the higher Mn doping.

## 2.7 Vapor Corrosion Inhibitors (VCIs)

Vapor Corrosion Inhibitors (VCIs), also sometimes called Vapor Phase Inhibitors (VPIs). VCIs are a group of assorted products which protect metal surfaces from attack by corrosive agents: moistures, salty air, airborne acids and

contaminants. VCI chemicals are a class of corrosion inhibiting organic compounds which have sufficient vapor pressure (about  $10^{-7}$ - $10^{-2}$ ) to release molecules from the compound into the air by diffusion through the gas phase and adsorbed onto the metal with a thickness of a few monolayers, thereby protecting it from corrosion. Corrosion of metal is an electro-chemical process; it begins when an electrolyte (water, oxygen, humidity) is present on the surface of a metal. When this happens, electrons then flow from high-energy areas of the metal to low-energy areas on a loop, through the electrolyte. The corrosion process results in the formation of oxidation on the metal surface. Volatile Corrosion Inhibitors retard this reaction by passivating the surface and inhibiting or depressing the electro-chemical mechanism that triggers oxidation, i.e., the current flow from anode to cathode. Electrical current attempts to flow from the anode through the electrolyte into the cathode but cannot because of the VCI's presence. VCI molecules attach themselves to a metal surface to form an invisible, thin film, possibly only a few molecules or even one molecule thick, to protect metal from attack. The efficiency of a compound used as VCI mainly depends on two parameters:

1. Its vapour pressure (more exactly: its tendency to sublime) under atmospheric conditions is high enough allowing significant vapour phase transport of the inhibitor within an enclosed space to the metal surface;
2. The VCI adsorbed directly on the metal surface or dissolved in a condensed water film on the metal surface inhibits the metal corrosion during storage and transport by interaction with the surface. (U. Rammelt *et al.*, 2009)

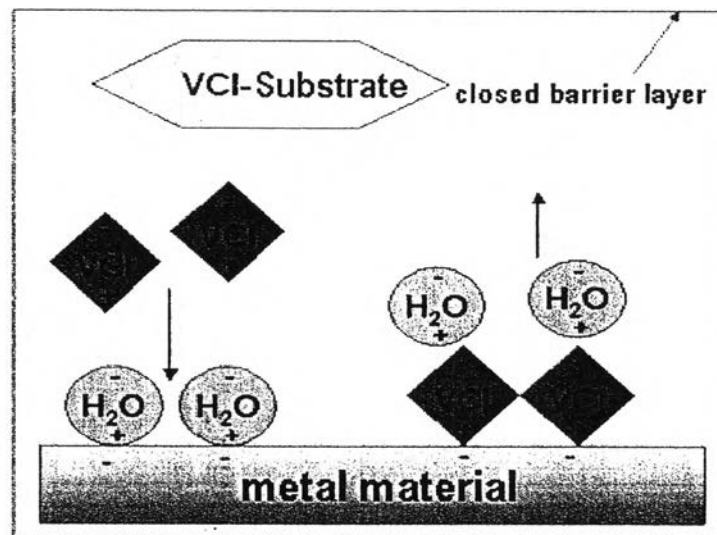


**Figure 2.10** The schematic of action of Vapor Corrosion Inhibitor.

([www.tisgdv.de/.../korrosio/schutz/schutz.htm](http://www.tisgdv.de/.../korrosio/schutz/schutz.htm))

#### **Advantages of the VCI method**

- Since the gas also penetrates holes and cavities, these areas also receive adequate protection.
- The period of action may extend to two years.
- The wrapping need not be provided with an airtight heat seal.
- On completion of transport, the packaged item need not be cleaned, but is immediately available.

#### **Disadvantages of the VCI method**

- The VCI method is not suitable for all metals. It may cause considerable damage to nonmetallic articles (plastics etc.).
- Most VCI active substances may present a hazard to health, so it is advisable to have their harmlessness confirmed by the manufacturer and to obtain instructions for use.

**Table 2.1** Examples of common inhibitor systems classified by their modes of action

Mode of action	Examples	
Adsorption	amines	$\text{RNH}_2$
	thiourea	$\text{NH}_2\text{CSNH}_2$
	Antimony trichloride	$\text{SbCl}_3$
	benzoate	$\text{C}_6\text{H}_5\text{COO}^-$
Passivating	nitrite	$\text{NO}_2^-$
	chromate	$\text{CrO}_4^{2-}$
	red lead	$\text{Pb}_3\text{O}_4$
	calcium plumbate	$\text{Ca}_2\text{PbO}_4$
Surface layer	phosphate	$\text{H}_2\text{PO}_4^-$
	silicate	$\text{H}_2\text{SiO}_4^{2-}$
	hydroxide	$\text{OH}^-$
	bicarbonate	$\text{HCO}_3^-$
	hexametaphosphate	$\text{Na}_6(\text{PO}_3)_6$

The examples of common inhibitor systems show in Table 2.1

The first classes of inhibitors are adsorption inhibitors are used quite widely in many proprietary mixtures which are marketed to control corrosion. For example, Amine inhibitors are sometimes present in volatile corrosion inhibitors. These are used in packaging materials to prevent corrosion of steel articles during transport.

The second classes of inhibitors are all oxidising agents, containing elements in their higher oxidation states. For example nitrite, which is used as an additive in cooling fluid circuits for the control of corrosion of steel, is a mild oxidising agent which can raise the potential of steel into the passivation region.

The last category of corrosion inhibitors are those which form a surface layer of a foreign chemical compound provided by the inhibitor itself. For example Hexametaphosphate functions as a corrosion inhibitor because it has a high affinity for metal cations such as calcium, zinc, copper and ferrous ions. Under some

conditions it acts to dissolve substances containing these cations and hence has a cleaning effect, assisting the removal of scale deposits. But at the surface itself an insoluble layer of a ferrous hexametaphosphate is deposited and will act as a corrosion inhibitor. (Graeme Wright)

U. Rammelt *et al.*, (2009) Some aspects of the passivation of mild steel in the presence of selected vapour phase corrosion inhibitors (VCI) were considered. In particular their ability to vapourize was evaluated by sublimation tests and their role in the inhibition mechanism of mild steel was investigated by electrochemical methods such as open circuit potential (OCP) and electrochemical impedance spectroscopy (EIS) measurements. In the presence of some carboxylates, amines and azoles alone and as mixtures a protective layer can be formed on mild steel in neutral and alkaline solution. It was shown that the passivation mechanism strongly depends on the pH of the solution. In addition the influence of contaminants from industrial alkaline cleaning baths on the protective properties was analyzed. The results show that also for ferrous metals protection by VCI in packages is more effective under neutral to slightly alkaline conditions than with strong alkaline conditions sometimes caused by the alkaline cleaning procedure.

K. L. Vasanth (1997) several commercially available VCI have been investigated on aluminum, steel and aluminum/steel (Al/steel) galvanic couple exposed to simulated marine environment using potentiation dynamic slow scans. The inhibitor efficiencies calculated from electrochemical data are presented. The systems reach a steady state after 48 hours of exposure of the metal to VCI vapors. The most efficient VCI were screened for toxicity before recommending them for selected ship-board applications in the U.S. Navy. The results show that electrochemical techniques have been used to study the performance of several water soluble corrosion inhibitors. However, such electrochemical study is scanty with regard to assessing the performance of VCI. The attempts to correlate the electrochemical measurements in a volume of electrolyte with actual atmospheric conditions occurring beneath thin films of electrolyte have been unsuccessful due to drastic changes in electrochemical behavior of metals under these two conditions<sup>5</sup>. It appears that for the first time an electrochemical study of VCI has been performed under conditions that are approximately intermediate between total immersion in



electrolyte and total marine atmospheric exposure - a condition that is experienced on top-side of a ship. And inhibitor efficiency is dependent on the type of metal/alloy, the type of environment, air-tightness of cabinets/enclosures in which they are placed, concentration and temperature fluctuations.

Niel Pieterse *et al.*, (2006) Volatile corrosion inhibitors (VCIs) are incorporated into packaging paper or film to protect metals against atmospheric corrosion. The vapour pressure determines the equilibrium concentration of a volatile corrosion inhibitor (VCI) in the surrounding atmosphere. However, the rate at which the VCI can be delivered across the air gap to a metal surface is determined by the gas permeability. The gas permeability of commercial VCIs was estimated at elevated temperatures from vaporisation rates measured using a simple thermogravimetric method (TG). Reasonable agreement between experiment and theory was obtained for scan rates between 2 and 20 °C/min when the 70 µl cup was filled to less than 50% of its volume at a gas flow rate of 50 ml/min. The results suggest that the permeability of tolyltriazole is comparable to that of dibutyl phthalate. At this stage the method can only provide order of magnitude comparisons at elevated temperatures for inert gas permeabilities of pure components.

Corrosion testing can be performed in the laboratory under controlled conditions and in the field under natural or service conditions. In both the laboratory and field tests, corrosion rate can be evaluated by the direct determination of the metal loss or by measuring of corrosion current, corrosion potential, polarization resistance, and other electrochemical corrosion characteristics with electrochemical instruments. It was shown that

- Use of Vapor Corrosion Inhibitors is a relatively new and is considered as a very effective corrosion protection technology.
- For performance evaluation of VCI containing products manufactures and end-users have to develop the testing program, which can include standard procedures and special tests, related to the service conditions as well.
- Results of outdoor and indoor study of a VCI Powder given in this work, situated at different distances from the metal, confirmed the effectiveness of VCI in corrosion protection for different metals under different set of conditions: buried in

sand, exposed to atmosphere, at high humidity and temperature ranges. (Alla Y. Furman *et al.*, 2004)

L.R.M. Esteveao *et al.*, (2001) study the modification of volatilization rate of volatile corrosion inhibitors by mean of host-guest system. TG/DTA analysis reveals that the volatility of thermally stable volatile corrosion inhibitors (VCIs) may be enhanced by their absorption on porous inorganic substrates such as zeolites and diatomaceous earths (DE). The corrosion testing results showed that all VCIs had their efficiency increased by zeolites and that the phosphate greatly benefitted from the use of DE.